Open Ceramics 19 (2024) 100636

Contents lists available at ScienceDirect

Open Ceramics

journal homepage: www.sciencedirect.com/journal/open-ceramics

Boron induced abnormal grain growth in alumina

Christian Bechteler [a,*], Hannes Kühl [b], Richard I. Todd [a]

[a] University of Oxford, Department of Materials, Parks Road, Oxford, OX1 3PH, UK
[b] Technische Hochschule Nürnberg Georg Simon Ohm, Fakultät Werkstofftechnik, Nürnberg, Germany

ARTICLE INFO

Handling Editor: Dr P Colombo

Keywords:
Alumina
Boron
Abnormal grain growth
Microstructure
Diffusion

ABSTRACT

In this work, hot-pressing of alumina in contact with hexagonal boron nitride or doped with boron carbide was conducted at 1500 °C for 30 min. After hot-pressing, abnormal grain growth induced by boron diffusion from these substances into alumina was detected, as clearly demonstrated with SEM, EDS, EBSD, and Raman spectroscopy. Grain boundary complexion transformations, solute drag, or another mechanism relating to interface-controlled grain boundary mobility are presumed to be the fundamental mechanism responsible for abnormal grain growth observed in this work.

1. Introduction

Ceramics are materials with outstanding properties, controlled and defined by their processing and final microstructure. Even though this connection has been well-known for decades, grain growth and microstructure evolution in alumina remain difficult to understand, particularly when grains grow abnormally fast, a phenomenon known as abnormal grain growth (AGG). One reason for this is the wide range of effects from different impurities.

It is known that AGG is not an intrinsic property of alumina (Al_2O_3) [1], which is the material most frequently used as a technical ceramic. However, if only a few ppm of certain impurities are present during sintering Al_2O_3 for several hours at temperatures above 1500 °C, AGG may occur [2–5]. AGG changes the fundamental microstructure and the overall properties of the material, making it important to investigate the conditions under which AGG happens.

Previous work on AGG in alumina, which mostly considers oxide impurities [2–5], has shown that liquid phase formation, doping with other impurities, solute drag, and various kinds of grain boundary complexions [4–8] play an important role and are potential mechanisms for AGG in alumina.

The work presented here investigates the possibility of boron (B) induced AGG in alumina caused by the presence of the non-oxides, specifically boron carbide (B_4C) and hexagonal boron nitride (hBN), during hot pressing in a graphite die in an inert atmosphere. The presence of hBN during hot pressing and its interaction with alumina is particularly interesting because hBN is often used as a protective layer on the graphite dies for pressure-assisted sintering.

2. Experimental

2.1. Materials and hot pressing

Pure alumina (TM-DAR, >99.99 % purity, D_{50} = 0.15 μm, Taimei Chemicals) was hot-pressed at 1500 °C in argon (Ar) for 30 min with a heating rate of 500 °C/h and an applied pressure of 80 MPa in a graphite (carbon) die. Half of the graphite bottom plate was replaced by a fully dense, high purity (TM-DAR, >99.99 % pure) alumina plate, which was pressureless sintered and had a grain size of 2 μm. The graphite bottom plate in contact with the alumina powder was ground and cleaned prior to sintering to remove any impurities. The graphite plate on top of the alumina powder and the inside of the surrounding die were coated with hexagonal boron nitride (hBN) spray (HeBoCoat SL-E 125, Henze BNP AG, Germany) as a protective layer, as is often done during hot-pressing. Based on this procedure, three different interfaces, alumina-alumina (Al_2O_3– Al_2O_3), alumina-carbon (Al_2O_3–C) and alumina-boron nitride (Al_2O_3-BN), are present, as shown in Fig. 1.

In addition, hot pressing of alumina containing 1 wt% of fractured boron carbide (B_4C) particles, ≈100 μm in size, was conducted under similar conditions to investigate the influence of B_4C on the microstructural evolution in alumina.

* Corresponding author.
E-mail address: christian.bechteler@wolfson.ox.ac.uk (C. Bechteler).

https://doi.org/10.1016/j.oceram.2024.100636
Received 28 April 2024; Received in revised form 21 June 2024; Accepted 4 July 2024
Available online 4 July 2024

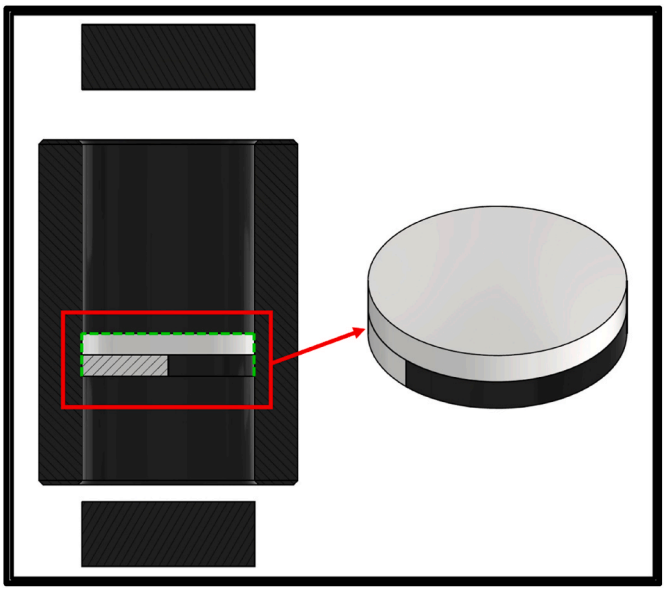

Fig. 1. Graphite die for hot-pressing of pure and doped alumina with a split bottom plate, half alumina, and half graphite (carbon). The top surface as well as surrounding area of the sample were in contact with the applied hexagonal boron nitride (hBN) layer, highlighted with a green dashed line.

2.2. Characterisation

Digital microscopy (KEYENCE VHX-6000 version 2.8.0.110) and SEM imaging, including EDS and EBSD (Merlin FEG SEM, Zeiss) were performed on fractured and polished surfaces of the samples, with some of them etched at 1100 °C for 15 min in air.

Polished surfaces were prepared by grinding and polishing the samples with colloidal silica.

Grain size measurements were performed using the linear interception method without applying a correction factor.

Raman spectroscopy on polished surfaces was conducted between 100 and 3200 cm^{-1}, using a red laser (633 nm).

3. Results

3.1. Microstructure at hot-pressed interfaces

The SEM images of the Al_2O_3–Al_2O_3-interface (red dashed lines in Fig. 2) show that the grains have overgrown the original interface, and that the microstructure of the previously sintered alumina and the hot-pressed alumina differ in GS. The GS is 1.5 μm for the hot-pressed part of the sample and 1.9 μm for the previously pressureless sintered plate. Furthermore, the microstructure shows some inter- and intragranular submicron pores where the pre-sintered disk and the hot-pressed part merge. Intragranular porosity mostly appears in grains at the interface,

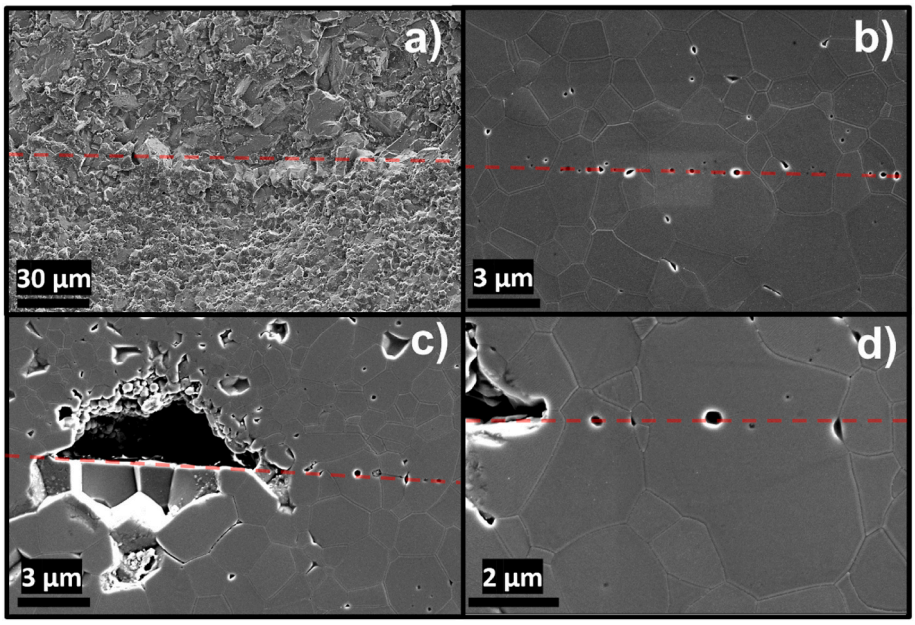

Fig. 2. SEM images of the fractured (a) and polished (b–d) Al_2O_3–Al_2O_3-interface including red dashed lines for visualisation of the actual interface between the pre-sintered disk and the subsequently hot-pressed material, which shows a few micrometre-sized pores (c) as well as submicron inter- and intragranular pores along the interface (b and d).

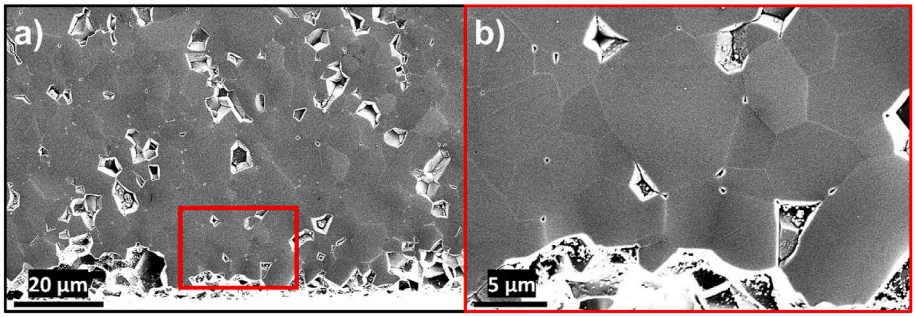

Fig. 3. Al_2O_3–C-interface of a hot-pressed Al_2O_3 ceramic, which was in direct contact with a cleaned graphite plate located at the bottom of the visualised microstructure; b) shows the in a) highlighted are at higher magnification which was in direct contact with the cleaned graphite plate.

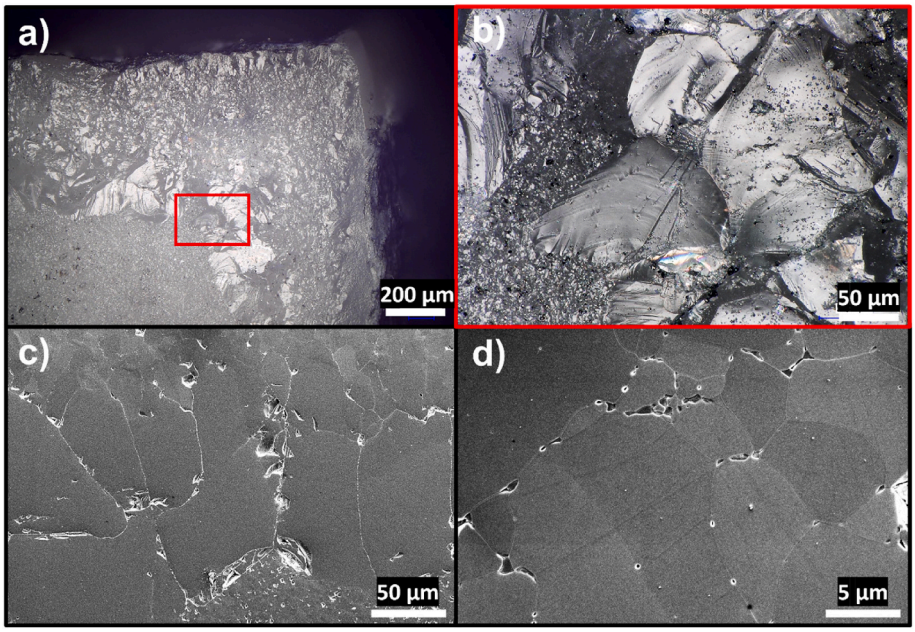

Fig. 4. Al_2O_3-hBN-interface of a hot pressed Al_2O_3 ceramic, which shows enhanced grain growth on the outer layer of the Al_2O_3 sample; b) shows the in a) highlighted fractured area; c) and d) show other polished areas with abnormally grown grains at various magnifications.

where some of these grains are comparatively large (>5 µm), but almost never within the pre-sintered disk or the hot-pressed part of the material, as shown in Fig. 2.

At the Al_2O_3–C-interface (Fig. 3), the microstructure, which has a grain size of 3.8 µm, shows enhanced grain growth compared to the Al_2O_3–Al_2O_3-interface region, but no other anomalies such as AGG are found. The enhanced grain growth at the Al_2O_3–C-interface can be explained by the (carbothermic) reduction [9] caused by the graphite die.

The grains located at the edge of the hot-pressed sample, shown in Fig. 4, where hBN was used as a separation layer between the Al_2O_3-powder and the graphite (carbon) die, show AGG, which is most obvious at 0.5 mm from the sample surface. This region represents the Al_2O_3-hBN-interface highlighted in Fig. 1. Grains in this region are up to several hundreds of micrometres in size, orders of magnitude larger than the normal sized grains (≈3 µm) that surround the abnormally grown grains.

3.2. Microstructure on B_4C–Al_2O_3-interface

Fig. 5 visualises a fractured (vertical) and perpendicular polished (horizontal) surface of an Al_2O_3-matrix showing abnormally grown Al_2O_3-grains surrounding a B_4C-particle.

The (not post-processed) EBSD map shown in Fig. 6 was taken on the polished surface around the B_4C particle and highlights the AGG with the orientation and size of the grains around the particle. A sharp transition from very large to small grains is clearly visible. Most large grains show a single orientation (one colour), though a few show two different orientations within one grain, which are always misoriented by 60°.

Furthermore, SEM images and EDS maps from the B_4C–Al_2O_3-interface, shown in Figs. 7 and 8, reveal the formation of a 1 µm thick interfacial region with high C-content, low amounts of O, but no Al. Due to its low atomic number, boron was not included in the EDS characterisation.

According to the Raman line scan shown in Fig. 9, which starts within the B_4C-particle, goes through the interface, and ends in the Al_2O_3-matrix, the following compositions are detected: I) pure B_4C, which can be seen in the Raman spectrum up to 1200 cm^{-1} (scan 1), II) B_4C with increased carbon-content (scan 2), III) pure carbon (scans 3 and 4), IV) carbon in Al_2O_3 (scans 5 to 8), and V) pure Al_2O_3 (scans 9 and 10).

Based on the measured Raman spectra, the pure carbon region (III) can be specified as 2D graphitic C-structure due to the strong D, G, D', and G' peaks shown in Fig. 9 c).

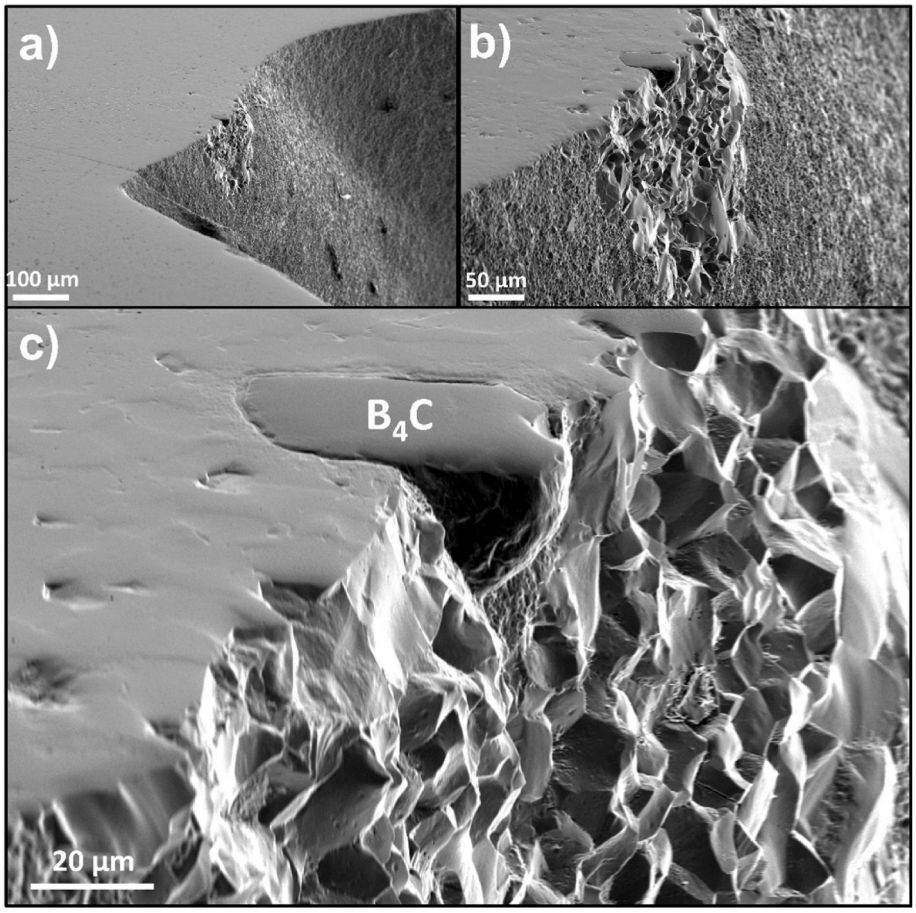

Fig. 5. SEM images at various magnifications (a–c) of a fractured and polished surface of an Al_2O_3 matrix including one solid particle of B_4C approx. 50 µm in diameter showing enhanced grain growth of alumina around the B_4C particle.

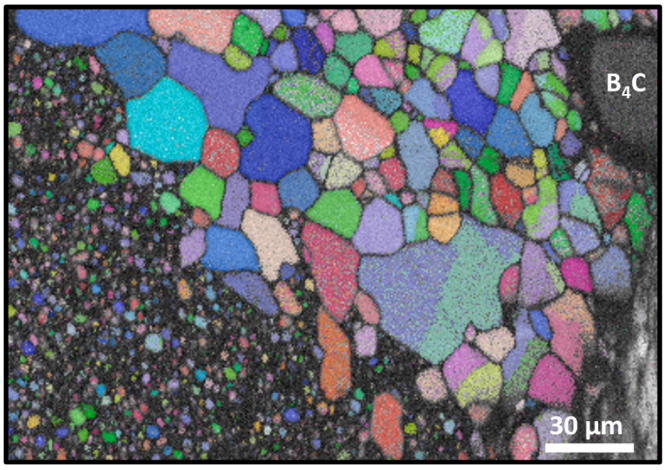

Fig. 6. EBSD map of the abnormally grown Al_2O_3-microstructure around a B_4C-particle located on the top right corner of the map shown in dark grey. Most grains show one orientation; however, some grains show two different regions, which are 60° misoriented towards each other.

4. Discussion

Since boron is difficult to detect by conventional methods such as EDS, particularly in low concentrations in the ppm range due to its low atomic number, it seems likely that the influence of boron on the Al_2O_3-microstructure has not been recognised until now, even though hBN is often used in hot-pressing, SPS, or other sintering techniques as a protective layer between graphite dies and Al_2O_3-powder.

The experiments conducted in this work show that if hexagonal boron nitride (hBN) or boron carbide (B_4C) is present and in direct contact with alumina (Al_2O_3), AGG of Al_2O_3 occurs during hot-pressing at 1500 °C for 30 min.

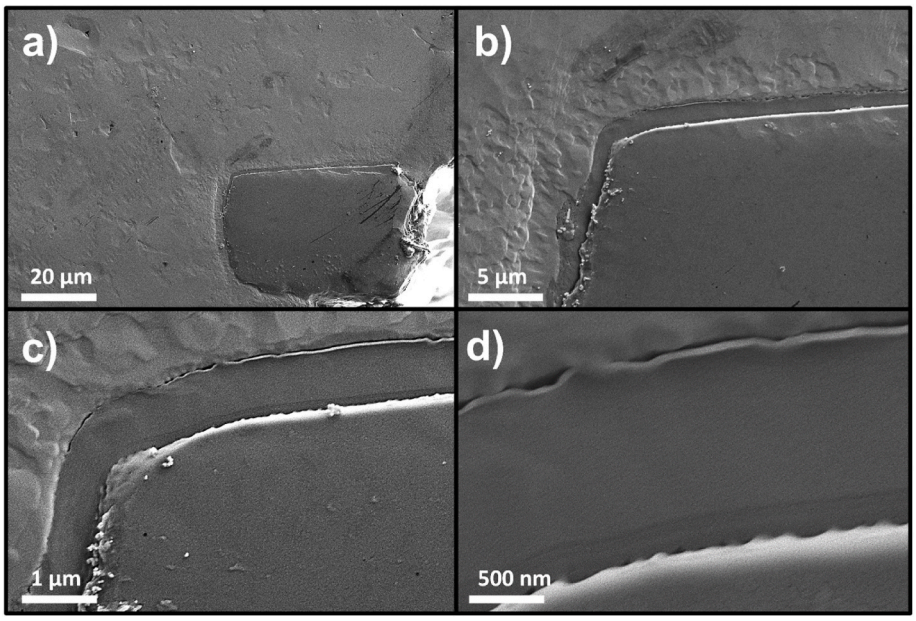

Fig. 7. SEM images of B_4C–Al_2O_3 interface after hot-pressing at various magnifications.

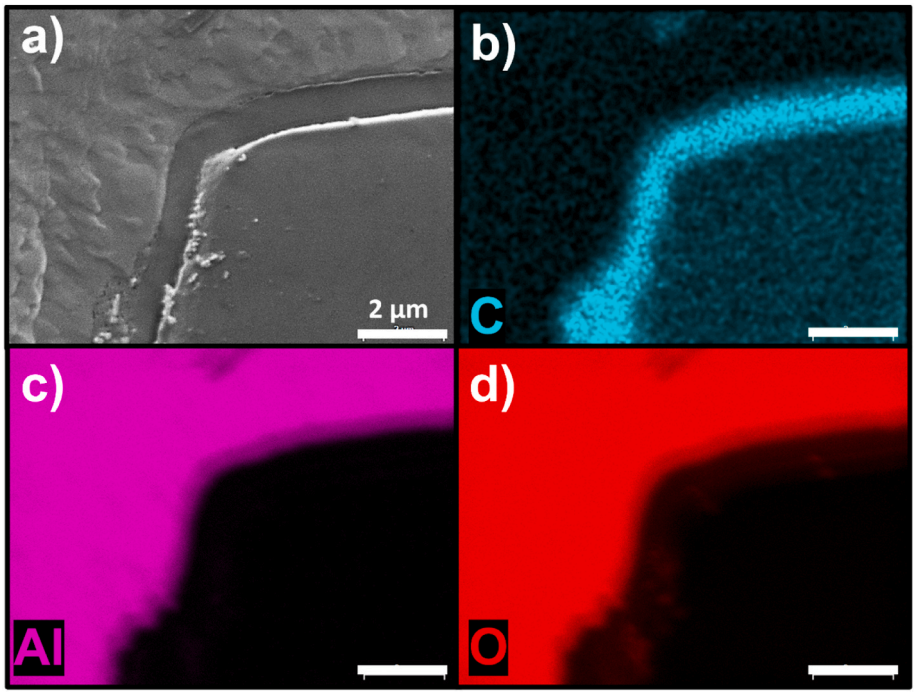

Fig. 8. a) SEM image of B_4C–Al_2O_3 interface after hot-pressing with the corresponding elemental distribution shown by EDS maps of b) carbon, c) aluminium and d) oxygen.

According to the literature, the fundamental mechanism for AGG under the present conditions is presumably related to the oxidation of B_4C and hBN, which typically occurs in two steps. First, the formation of B_2O_3, which increases rapidly at temperatures above 1200 °C [10]. Second, the subsequent evaporation of B_2O_3, which increases sharply above 1300 °C [10,11]. Since these reactions occur below the temperatures usually applied during sintering of Al_2O_3 in air, boron-containing substances oxidise, and the formed boron oxide evaporates during the sintering process of Al_2O_3 in air.

However, if no atmospheric oxygen is available to oxidise B_4C or hBN, the oxidation and evaporation process is limited because B_4C and hBN do not evaporate at temperatures around 1500 °C. The results presented here suggest a reaction of B_4C or hBN with the oxygen contained in alumina and the diffusion of boron (B) along grain boundaries, which leads to a depletion of B in some of the regions that were originally B_4C or hBN, as was shown in this work for B_4C, which was surrounded by an almost pure layer of (2D-)carbon.

The diffusion of B into alumina could lead to liquid phase formation, which begins at significantly lower temperatures [12–14] than those required for the densification of Al_2O_3 and the applied sintering temperature of 1500 °C. It is known from other substances such as CaO [3], SiO_2, and TiO_2 that the presence of liquid phases can induce AGG in

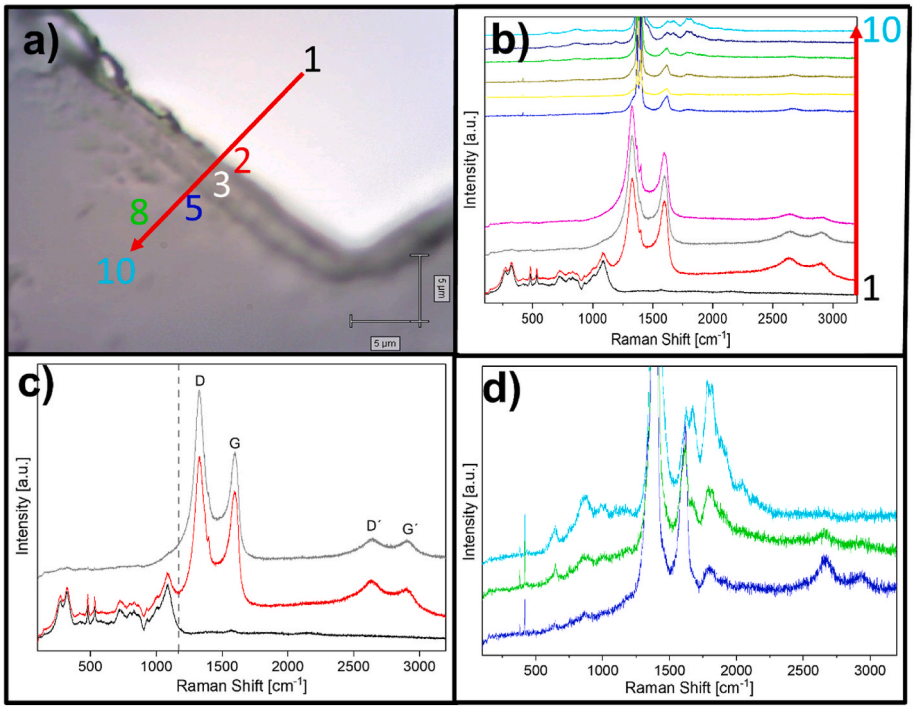

Fig. 9. Raman Spectra obtained from the B_4C–Al_2O_3 interface after hot-pressing starting at the interior of the B_4C particle (1) reaching into Al_2O_3 (10). a) shows the microscope image of the investigated region with the B_4C particle as bright area; b) shows all the 10 line-scan spectra; c) shows the scans 1–3 located in the B_4C particle (1) as well as the C-rich interfacial layer (3); d) shows the scans 5 (dark blue), 8 (green) and 10 (light blue) taken on the Al_2O_3 matrix side.

Al_2O_3 [1,2,4]. Other impurity-related effects can also stimulate AGG, including of the formation of particularly mobile grain boundary complexions, solute drag, and other interface-control effects that induce non-linearity in the grain boundary velocity versus driving force relationship which are possible mechanisms for AGG [5–8,15].

From previous investigations conducted under different circumstances, such as sintering in air and higher concentrations of boron-containing substances, it is known that composites made from B_2O_3 and Al_2O_3 can also form elongated aluminium borate grains or whiskers [16–20]. Furthermore, B_2O_3 is suitable for generating strong joints between Al_2O_3 ceramics [21,22]. However, grains or structures with high aspect ratios were not observed in this work. This is likely due to the different approaches and experimental conditions. Nevertheless, it shows that various effects in Al_2O_3 can originate from the presence of substances or impurities such as B_2O_3.

5. Conclusions

The research conducted here showed that boron-containing substances such as hexagonal boron nitride or boron carbide induce abnormal grain growth in alumina during hot-pressing at 1500 °C for 30 min in an inert atmosphere. This phenomenon is presumed to be caused by the diffusion of boron into the alumina matrix.

CRediT authorship contribution statement

Christian Bechteler: Writing – review & editing, Writing – original draft, Methodology, Investigation, Funding acquisition, Data curation, Conceptualization. **Hannes Kühl:** Writing – review & editing, Validation, Supervision, Resources, Methodology, Investigation, Funding acquisition, Data curation, Conceptualization. **Richard I. Todd:** Writing – review & editing, Validation, Supervision, Resources, Methodology, Investigation, Funding acquisition, Data curation, Conceptualization.

Declaration of competing interest

The authors declare that they have no known competing financial interests or personal relationships that could have appeared to influence the work reported in this paper.

Acknowledgements

This work was supported by the Engineering and Physical Sciences Research Council [EP/T517811/1] and the Studienstiftung des deutschen Volkes – German Academic Scholarship Foundation. The authors acknowledge use of characterisation facilities within the David Cockayne Centre for Electron Microscopy, Department of Materials, University of Oxford, alongside financial support provided by the Henry Royce Institute (Grant ref EP/R010145/1).

References

[1] I.J. Bae, S. Baik, Abnormal grain growth of alumina, J. Am. Ceram. Soc. 80 (5) (1997) 1149–1156, https://doi.org/10.1111/J.1151-2916.1997.TB02957.X.
[2] Y. Kim, S. Hong, D. Kim, Anisotropic abnormal grain growth in TiO2/SiO2-doped alumina, J. Am. Ceram. Soc. 83 (11) (Nov. 2000) 2809–2812, https://doi.org/10.1111/j.1151-2916.2000.tb01636.x.
[3] J. Jung, S. Baik, Abnormal grain growth of alumina: CaO effect, J. Am. Ceram. Soc. 86 (4) (2003) 644–649, https://doi.org/10.1111/J.1151-2916.2003.TB03353.X.
[4] S. Hong, D. Kim, Effect of liquid content on the abnormal grain growth of alumina, J. Am. Ceram. Soc. 84 (7) (Jul. 2001) 1597–1600, https://doi.org/10.1111/j.1151-2916.2001.tb00883.x.
[5] S.J. Dillon, S.K. Behera, M.P. Harmer, An experimentally quantifiable solute drag factor, Acta Mater. 56 (6) (Apr. 2008) 1374–1379, https://doi.org/10.1016/j.actamat.2007.11.042.
[6] P.R. Cantwell, S. Ma, S.A. Bojarski, G.S. Rohrer, M.P. Harmer, Expanding time–temperature-transformation (TTT) diagrams to interfaces: a new approach for grain boundary engineering, Acta Mater. 106 (Mar. 2016) 78–86, https://doi.org/10.1016/j.actamat.2016.01.010.
[7] S.A. Bojarski, M.P. Harmer, G.S. Rohrer, Influence of grain boundary energy on the nucleation of complexion transitions, Scripta Mater. 88 (Oct. 2014) 1–4, https://doi.org/10.1016/j.scriptamat.2014.06.016.
[8] S.G. Kim, Y.B. Park, Grain boundary segregation, solute drag and abnormal grain growth, Acta Mater. 56 (15) (Sep. 2008) 3739–3753, https://doi.org/10.1016/j.actamat.2008.04.007.

[9] Y. Dong, H. Wang, I.-W. Chen, Electrical and hydrogen reduction enhances kinetics in doped zirconia and ceria: I. grain growth study, J. Am. Ceram. Soc. 100 (3) (Mar. 2017) 876–886, https://doi.org/10.1111/jace.14615.
[10] V.A. Lavrenko, A.F. Alexeev, High-temperature oxidation of boron nitride, Ceram. Int. 12 (1) (Jan. 1986) 25–31, https://doi.org/10.1016/S0272-8842(86)80006-2.
[11] M. Steinbrück, Oxidation of boron carbide at high temperatures, J. Nucl. Mater. 336 (2–3) (Feb. 2005) 185–193, https://doi.org/10.1016/J.JNUCMAT.2004.09.022.
[12] H.F. Rizzo, Oxidation of boron at temperatures between 400 and 1300°C in air, in: Boron Synthesis, Structure, and Properties, Springer US, Boston, MA, 1960, pp. 175–189, https://doi.org/10.1007/978-1-4899-6572-1_21.
[13] A. Jain, K. Joseph, S. Anthonysamy, G.S. Gupta, Kinetics of oxidation of boron powder, Thermochim. Acta 514 (1–2) (Feb. 2011) 67–73, https://doi.org/10.1016/j.tca.2010.12.004.
[14] Y. Zhu, J. Cai, N.S. Hosmane, Y. Zhang, Introduction: basic concept of boron and its physical and chemical properties, in: Fundamentals and Applications of Boron Chemistry, Elsevier, 2022, pp. 1–57, https://doi.org/10.1016/B978-0-12-822127-3.00003-X.
[15] J.G. Fisher, S.L. Kang, Strategies and practices for suppressing abnormal grain growth during liquid phase sintering, J. Am. Ceram. Soc. 102 (2) (Feb. 2019) 717–735, https://doi.org/10.1111/jace.16008.
[16] L.A. Xue, I. Chen, Low-temperature sintering of alumina with liquid-Forming additives, J. Am. Ceram. Soc. 74 (8) (Aug. 1991) 2011–2013, https://doi.org/10.1111/j.1151-2916.1991.tb07825.x.
[17] Z. Misirli, H. Erkalfa, O.T. Özkan, Effect of B2O3 addition on the sintering of α-Al2O3, Ceram. Int. 22 (1) (Jan. 1996) 33–37, https://doi.org/10.1016/0272-8842(95)00050-X.
[18] P.O. Ike, et al., The effect of copper on the structural and thermoluminescence properties of aluminium borate, J. Lumin. 226 (Oct. 2020) 117504, https://doi.org/10.1016/j.jlumin.2020.117504.
[19] Y. Liu, Q. Li, S. Fan, Self-catalytic growth of aluminum borate nanowires, Chem. Phys. Lett. 375 (5–6) (Jul. 2003) 632–635, https://doi.org/10.1016/S0009-2614(03)00930-8.
[20] K. Suganuma, T. Fujita, N. Suzuki, K. Niihara, Aluminium composites reinforced with a new aluminium borate whisker, J. Mater. Sci. Lett. 9 (6) (Jun. 1990) 633–635, https://doi.org/10.1007/BF00721787.
[21] L.-L. Zhu, et al., Alumina ceramics joined with screen-printed B2O3 by spark plasma sintering, Ceram. Int. 47 (21) (Nov. 2021) 30838–30843, https://doi.org/10.1016/j.ceramint.2021.07.264.
[22] W. Guo, T. Lin, P. He, Microstructure and mechanical property of sapphire joints reinforced byAl4B2O9 whiskers, J. Mater. Res. Technol. 12 (May 2021) 739–748, https://doi.org/10.1016/j.jmrt.2021.03.042.